

# A Semiparametric Deconvolution Model to Establish In Vivo–In Vitro Correlation Applied to OROS Oxybutynin

MARIA PITSIU,<sup>1</sup> GAYATRI SATHYAN,<sup>2</sup> SUNEEL GUPTA,<sup>2</sup> DAVIDE VEROTTA<sup>1,3</sup>

<sup>1</sup>Department of Biopharmaceutical Sciences, School of Pharmacy, University of California, Bos 0446, San Francisco, California 94143-0446

<sup>2</sup>Alza Corporation, Mountain View, California 94043

<sup>3</sup>Department of Epidemiology and Biostatistics, University of California, San Francisco, California 94143

Received 6 July 1999; revised 26 September 2000; accepted 28 September 2000

**ABSTRACT:** *In vitro*–*in vivo* correlation (IVIVC) models may be used to predict *in vivo* drug concentration–time profiles given *in vitro* release characteristics of a drug. This prediction is accomplished by incorporating *in vitro* release characteristics as an input function ( $A_{\text{vitro}}$ ) to a pharmacokinetics model. This simple approach often results in biased predictions of observed *in vivo* drug concentrations, and it can result in rejecting IVIVC. To solve this problem we propose a population IVIVC model that incorporates the *in vitro* information and allows one to quantify possibly changed *in vivo* release characteristic. The model assumes linear kinetics and describes the *in vivo* release as a sum of  $A_{\text{vitro}}$  and a nonparametric function ( $A_d$ , a spline) representing the difference in release due to *in vivo* conditions. The function  $A_{\text{vitro}}$  and its variability enter the model as a prior distribution. The function  $A_d$  is estimated together with its intersubject variability. The number of parameters associated with  $A_d$  defines the model: no parameters indicates perfect IVIVC, a large number of parameters indicates poor IVIVC. The number of parameters is determined using statistical model selection criteria. We demonstrate the approach to solve the IVIVC problem of an oral extended release oxybutynin form (OROS), administered in three pharmacokinetic studies. These studies present a particular challenging case; that is, the relative bioavailability for the OROS administration is >100% compared with that of the immediate-release form. The result of our modeling shows that the apparent lack of IVIVC can be overcome: *in vivo* concentration can be predicted (within or across data sets) based on *in vitro* release rate together with a simple form of systematic deviation from the *in vitro* release.

© 2001 Wiley-Liss, Inc. and the American Pharmaceutical Association *J Pharm Sci* 90:702–712, 2001

**Keywords:** linear systems; controlled release; clinical study; validation data

## INTRODUCTION

*In vitro*–*in vivo* correlation (IVIVC) models are used to predict the *in vivo* drug concentration–time profiles given *in vitro* release characteristics

of a drug within certain specifications. To use terminology that might be familiar to people working in the IVIVC field, a IVIVC model is concerned with “Level A” correlation: that is, comparing the dissolution and absorption profiles to assess their degree of similarity (and therefore the similarity of the corresponding drug concentration predictions). The simplest IVIVC model assumes linearity with dose and stationarity (time invariance) with time, and predicts concentrations using drug release in place of drug

---

Correspondence to: D. Verotta (Telephone: 415-476-1556; Fax: 415-476-1556; E-mail: davide@ariel.ucsf.edu)

*Journal of Pharmaceutical Sciences*, Vol. 90, 702–712 (2001)  
© 2001 Wiley-Liss, Inc. and the American Pharmaceutical Association

absorption. A recent collection of contributions on the topic can be found in Young et al.<sup>1</sup>

The main IVIVC modeling problems are how to (i) incorporate the information on the *in vitro* release rates (see Langenbucher<sup>2</sup> for a basic model), (ii) take into account the possibly changed *in vivo* release characteristic of a formulation, (iii) take into account absorption and disposition kinetics (taking place between the release site(s) and the observation site), (iv) incorporate the variability associated with the *in vitro* release rates, and (v) take into account interindividual variability in *in vivo* release (and absorption/disposition).

Most approaches currently available do not address these problems simultaneously. In this paper we do, starting from the general modeling framework described by Verotta<sup>3</sup> to further develop a semiparametric model that addresses problems (i)–(v) for the case of a linear pharmacokinetics system. The semiparametric model we propose is based on the introduction of a “fudge function,” which empirically corrects the difference between (*in vitro*) release and (*in vivo*) absorption, and allows IVIVC-type predictions. The fudge function can range from the zero function, indicating perfect IVIVC, to a really flexible function, indicating poor IVIVC. Determining the flexibility of the fudge function is crucial to determining the extent of IVIVC and to obtaining unbiased IVIVC type predictions. We use statistical model selection criteria to determine this flexibility.

We apply the model to solve the IVIVC problem of an oral extended-release oxybutynin form (OROS) administered in different formulations and under different conditions in three different studies. These studies present a particular challenging case of IVIVC; that is, the relative bioavailability for the controlled-release administration is >100% compared with that of the immediate-release (IR) form.<sup>4</sup> This observation suggests that the drug metabolism/transport of the drug is different between the two formulations and implies that a naive application of IVIVC (where *in vitro* release rates are used to predict concentrations) would fail to represent the OROS data.

The paper is organized as follows: (i) description of the oxybutynin studies, (ii) the details of the model used for IVIVC together with the method used to estimate its parameters and select the fudge function, (iii) the IVIVC results, and (iv) a discussion.

## METHODS

Three pharmacokinetics studies were conducted in healthy subjects. Concentration–time data of plasma *R*- and *S*-oxybutynin concentration after administration of either IR or controlled-release (OROS) racemic oxybutynin were collected. The two enantiomers were measured separately. The three studies (indicated by the symbols A, B, and C in the following) are fully described by Sathyan et al.,<sup>5,6</sup> and we briefly summarize them here for easy reference.

### Relative Bioavailability Study (Study A)

Forty-one subjects received the following treatments: IR oxybutynin, 15 mg (5 mg every 8 hr under fasting conditions); OROS,  $1 \times 10$  mg (under fasting conditions, this treatment will be indicated by the symbol *R*-1\_A or *S*-1\_A, where *R* and *S* indicate the enantiomer); OROS,  $1 \times 10$  mg (under fed conditions; *R*- or *S*-2\_A); and OROS,  $2 \times 5$  mg (under fasting conditions; *R*- or *S*-3\_A (OROS formulations were administered as a single dose at 8:00 a.m.; the IR formulation was administered at 8:00 a.m. or 12:00 p.m.)

### Dose Proportionality Study (Study B)

Subjects received only OROS treatments, all as a single dose at 8:00 a.m. under fasting conditions: OROS,  $2 \times 5$  mg (35 subjects; *R*- or *S*-1\_B); OROS,  $1 \times 10$  mg (36 subjects; *R*- or *S*-2\_B); OROS,  $4 \times 5$  mg (35 subjects; *R*- or *S*-3\_B).

### Bioequivalence Study (Study C)

Subjects received only OROS treatments, all as a single dose at 8:00, under fasting conditions: OROS,  $1 \times 10$  mg, commercial formulation (54 subjects; *R*- or *S*-1\_C); OROS,  $1 \times 10$  mg, clinical formulation (52 subjects; *R*- or *S*-2\_C).

Information about the *in vitro* release for all the formulations used was given by mean release rates and their standard deviations (see Figure 1). A standard USP VII apparatus was used for the experiment. The experiment lasted 24 h (and therefore there was no information on the *in vitro* release rate after that time). We assigned zero *in vitro* release rate for times  $\geq 24$  h.

## MODELS

The starting point of our approach is the convolution operator, which, for a linear pharmacokinetics

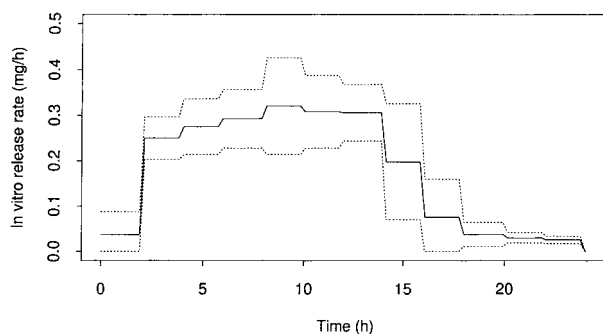


**Figure 1.** *R- or S-oxybutynin in vitro* release rate from a 10-mg OROS formulation. Key: (solid line) mean rate; (dotted lines)  $\pm$  one standard deviation.

system, obtains predicted concentration at a site (for example plasma) given the disposition function of the site ( $K(t)$ ) and the input rate to the site ( $A(t)$ ) (see Verotta<sup>7</sup> for a review). The convolution operator intertwines  $K$  and  $A$  to obtain drug concentration at an arbitrary time  $t$  ( $C(t)$ ) as follows:

$$C(t) = \int_0^t A(\tau)K(t - \tau)d\tau \quad (1)$$

where  $t = 0$  marks the beginning of the input, and  $\tau$  is an integration variable. To simplify notation, we will indicate convolution using the asterisk (\*) symbol. Using this notation, eq. 1 becomes  $C = A * K$ . We remark that the bioavailability (BIO) is obtained from eq. 1 as total input divided by the dose (Dose):

$$\text{BIO} = \frac{\int_0^\infty A(\tau)d\tau}{\text{Dose}} \quad (2)$$

### IR Disposition Function

The pharmacokinetics of racemic oxybutynin in humans after oral administration of an IR formulation or a solution have been best described by a first-order absorption and a two-compartment disposition.<sup>8</sup> In the experiments we use to demonstrate our approach to IVIVC, absorption and disposition cannot be independently determined (one would need an intravenous administration to do so). Therefore, the function  $K(t)$  in eq. 1 combines absorption and disposition, representing the response following a unit IR dose (IR disposition function). For convenience, we used the following parametrization for the IR disposition

function

$$K(t) = (k_a e^{-k_a t}) * (\beta_1 e^{-\beta_2 t} + \beta_3 e^{-\beta_4 t}) \quad (3)$$

(Note that using this parametrization, the bioavailability for the IR formulation is not explicitly stated but is incorporated in the “intercept”  $\beta_1 + \beta_3$ , which equals the ratio bioavailability divided by plasma volume.)

### Input Function and IVIVC

A naive solution to the IVIVC problem simply uses the available information on *in vitro* release rate ( $A_{\text{vitro}}$ ) in place of  $A$ , and predicts  $C$  using:

$$C = A_{\text{vitro}} * K \quad (4)$$

where  $K$ , for simplicity, again includes absorption and disposition. To take into account the systematic deviation between *in vitro* release and *in vivo* release, we propose to use an additive model of the form:

$$A_{\text{vivo}} = A_{\text{vitro}} + A_d \quad (5)$$

where  $A_{\text{vivo}}$  is the *in vivo* release rate function and  $A_d$  indicates an unknown function of time. The parameter  $A_d$  modifies  $A_{\text{vitro}}$  to account for the overall changes induced by the *in vivo* conditions. In the present applications, the model, depicted in Figure 2, takes the form:

$$C = (A_{\text{vitro}} + A_d) * K \quad (6)$$

We use longitudinal splines<sup>9</sup> to represent  $A_{\text{vitro}}$  and  $A_d$ .<sup>(1)</sup> For the  $k$ th individual, the inputs in the model are represented as follows:

$$A_{\text{vitro}}(t) = \sum_i \gamma_{i,\text{vitro}} B_{i,\text{vitro}}(t) \quad (7)$$

<sup>(1)</sup>A spline<sup>10</sup> is characterized by a sequence of distinct and nondecreasing real numbers called breakpoints. The polynomials making up a spline join at the breakpoints and satisfy there certain continuity conditions. For example, for a linear spline, the polynomials simply join at the breakpoints. For a cubic spline, the polynomials join and so do their first and second derivatives. A spline can be represented as a sum of basis functions,  $B(t)$ , each multiplied by a parameter ( $\gamma_i$ ). We indicate such sums as  $\sum_i \gamma_i B_i(t)$  where  $\sum_i$  indicates summation from  $i$  equal one to the number of basis functions in the spline. Different basis functions are associated with different sequences of breakpoints.

which is the formulation-specific *in vitro* release rate, where we omit, for clarity, a subscript indicating a specific formulation, and

$$A_d(t) = \sum_j \gamma_{jk,d} B_{j,d}(t) \tag{8}$$

where  $B_{i,\text{vitro}}$  and  $B_{j,d}^{(1)}$  are the spline bases for  $A_{\text{vitro}}$  and  $A_d$ , respectively, and the parameters of the splines take the form

$$\gamma_{i,\text{vitro}} = \delta_{i,\text{vitro}} e^{\eta_{i,\text{vitro}}} \tag{9}$$

$$\gamma_{j,kd} = \delta_{j,d} e^{\eta_{j,d}} \tag{10}$$

where  $\delta_{i,\text{vitro}}$  and  $\delta_{i,d}$  are fixed effects, and  $\eta_{i,\text{vitro}}$  and  $\eta_{i,d}$  are normally distributed random effects with mean zero and variance-covariance matrix  $\Omega_{\text{vitro}}$  and  $\Omega_d$ , respectively. The random effects represent individual departure from the parameters  $\delta_{i,\text{vitro}}$  and  $\delta_{j,d}$ . The model for  $k$ th individual takes the form:

$$\begin{aligned} C &= (A_{\text{vitro}} + A_d) * K_k \\ &= \left( \sum_i \gamma_{i,\text{vitro}} B_{i,\text{vitro}}(t) + \sum_j \gamma_{jk,d} B_{j,d}(t) \right) * K_k(t) \end{aligned} \tag{11}$$

where  $K_k$  indicates the IR disposition function for the  $k^{\text{th}}$  individual (characterized by individual specific parameters  $ka_k$ , and  $\beta_{ik}, i = 1, \dots, 4$ ). We used a zero-order spline (piecewise constant polynomial) for  $A_{\text{vitro}}$ , and a first-order spline (piecewise linear polynomial) for  $A_d$ .

**Estimation**

In the model fitted to the data from study A, we estimated the parameters  $\delta_{i,d}$  and the (diagonal) variance covariance matrix  $\Omega_d$  conditional on:  $\delta_{j,\text{vitro}}$  and  $\Omega_{\text{vitro}}$  (obtained from the *in vitro* experiment), and the parameters  $ka_k$  and  $\beta_{ik}$  (obtained from the IR experiment, subject to the constraint  $ka_k \geq \beta_{2k} \geq \beta_{4k}$ ). The parameters  $\delta_{i,d}$  are constrained to be non-negative, which implies that  $A_d$  is non-negative (as it is always the case for

<sup>(2)</sup>We will use the notation  $O_i$  to indicate the collection of objects  $O_1, O_2, \dots$ . This notation is used to simplify notation. Using this convention,  $B_{i,\text{vitro}}$  will indicate the collection of basis  $B_{1,\text{vitro}}, B_{2,\text{vitro}}, \dots$ . The identification of individual objects will be made clear by the context. For example, in  $\sum_i \gamma_i B_i(t)$ ,  $\gamma_i$  and  $B_i$  indicate the  $i^{\text{th}}$  parameter and basis, respectively, not their collections.

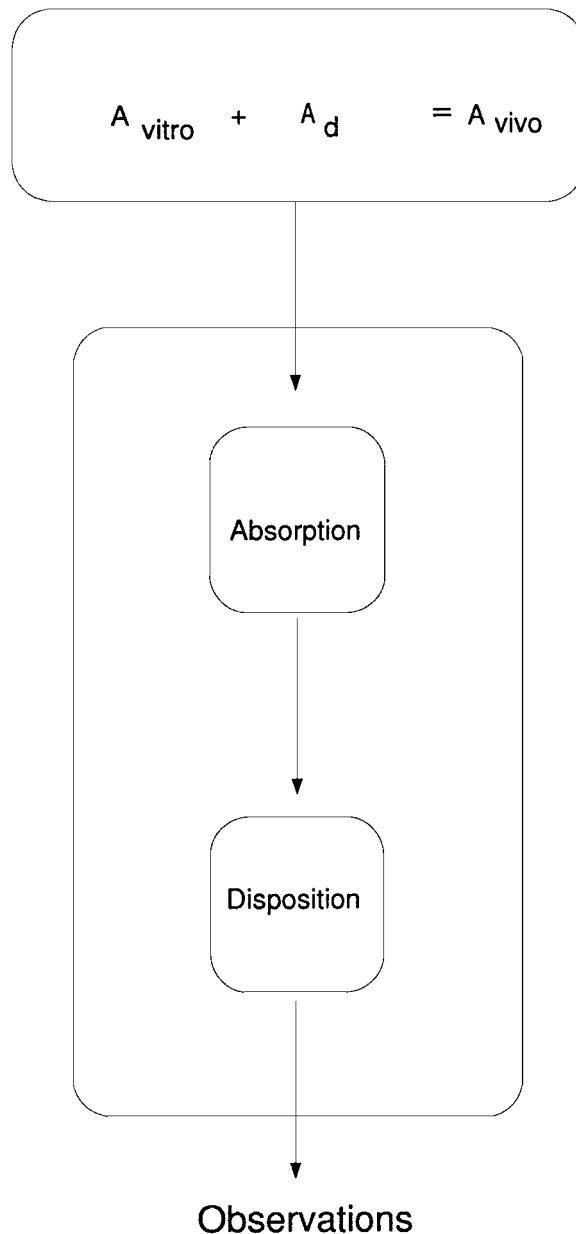


**Figure 2.** The conceptual model for IVIVC.

the OROS data). The term  $A_{\text{vivo}}$  is therefore non-negative as a sum of two non-negative functions (as it should for physical realism). This model is called M2 in the following. For comparison, we also consider model M1, which assumes  $A_{\text{vivo}} \equiv A_{\text{vitro}}$ .

One additional model, M3, was used for the data from study B and C in which the individual subjects IR disposition functions were not available. In model M3, we estimated  $\delta_{i,d}$  and  $\Omega_d$  conditional on:  $\delta_{j,\text{vitro}}$ ,  $\Omega_{\text{vitro}}$  and the population

mean of the parameters  $\beta_{ik}$  and  $k\alpha_k$  obtained from the IR experiment in study A.

All data analyses were conducted using NONMEM<sup>11</sup> and the FOCE method. Empirical Bayes estimates for individual subjects were obtained using the POSTHOC option. In all models, intra-subject variability (measurement error) was assumed to be proportional to the predicted concentration.

### Model Selection

The number of breakpoints used to define  $A_d$  corresponds to its number of parameters (or “dimension”), and it is proportional to the “flexibility” of  $A_d$ . With two breakpoints,  $A_d$  is a straight line. A larger number of breakpoints indicates a progressively more complex systematic deviation between *in vitro* and *in vivo* release. We tried 2–5 breakpoints equispaced between 0 and 48 h, which correspond to 2–5 parameters in  $A_d$ . To choose the number of breakpoints (and model M1 versus M2), we used the Akaike<sup>12</sup> criterion (AKA). Alternative asymptotic or data-based (cross-validation or test sets) model selection criteria can of course be used. (More conservative criteria<sup>13,14</sup> obtain the same results as the AKA for the data sets considered here.)

### Alternative Parametrization

The parametrization just presented is of general applicability. However, when the *in vivo* absorption is smaller than the *in vitro* release, one needs to use a less stringent constraints. We used  $A_d \geq 0$  and  $A_{\text{vitro}} \geq 0$ , which implies  $A_{\text{vivo}} \geq 0$ , and the implicit constraint  $A_{\text{vivo}} \geq A_{\text{vitro}}$ , which is appropriate for the data considered here. However, the less stringent constraint  $A_{\text{vivo}} \geq 0$  (which does not imply either  $A_{\text{vivo}} \geq A_{\text{vitro}}$  or  $A_{\text{vivo}} \leq A_{\text{vitro}}$ ), is difficult to impose in NONMEM. In these cases, the following alternative representation can be used:

$$A_{\text{vivo}} = A_{\text{vitro}} A_d \quad (12)$$

where  $A_{\text{vitro}}$  and  $A_d$  are constrained to be non-negative. Using these constraints  $A_{\text{vivo}}$  is non-negative, but  $A_{\text{vivo}}$  can be either greater or smaller than  $A_{\text{vitro}}$ .

### Summary Parameters

To compare results, we computed the following total absorption parameters: the integral of  $A_{\text{vitro}}$

from 0 to 48 h ( $A_{\text{VITRO}}$ ); the integral of  $A_d$  from 0 to 48 h ( $A_D$ ); and the integral (total input) of  $A_{\text{vivo}}$  from 0 to 48 h ( $A_{\text{VIVO}}$ ). The relative bioavailability (BIO) was computed as the ratio of  $A_{\text{VIVO}}$  to the corresponding nominal dose. We also computed the input rates at 12 and 24 h for  $A_d$  ( $A_{d,12}$  and  $A_{d,24}$ , respectively),  $A_{\text{vivo}}$  ( $A_{\text{vivo},12}$  and  $A_{\text{vivo},24}$ , respectively), and  $A_{\text{vitro}}$  (for which only  $A_{\text{vitro},12}$  is reported because  $A_{\text{vitro},24}$  is always zero, see Figure 1).

## RESULTS

### Disposition Function (IR Data, Study A)

In the IR data there appeared to be some difference in the maximum plasma concentrations and the area under the curve of concentration–time between the morning and the evening administration profiles for both enantiomers, with the levels for the 4:00 a.m. doses being on average lower than those of other doses. At a preliminary stage, the possibility of modeling the (apparent) IR absorption rate and relative bioavailability fraction as time-variant parameters was investigated, but the evidence for time dependence was inconclusive for these data (some subjects showed some evidence of possible time variance but most did not) and we decided to assume time invariance.

The mean estimated ( $\pm$  standard deviation, SD) IR disposition parameters for *R*-oxybutynin were  $k_a$  (L/h), 3.75 ( $\pm$  7.98);  $\beta_1$  (L/mL), 0.799 ( $\pm$  0.54);  $\beta_2$  (L/h), 0.932 ( $\pm$  0.453);  $\beta_3$  (L/mL), 0.67 ( $\pm$  0.088); and  $\beta_4$  (L/h), 0.157 ( $\pm$  0.261). The mean ( $\pm$  SD) IR disposition parameters for *S*-oxybutynin were  $k_a$ , 12.02 ( $\pm$  14.72);  $\beta_1$  17.76 ( $\pm$  89.22);  $\beta_2$ , 6.059 ( $\pm$  26.75);  $\beta_3$  0.141 ( $\pm$  0.087); and  $\beta_4$  0.102 ( $\pm$  0.080).

### In Vivo Input Function (OROS Data, Study A)

Model M2 provided a vastly superior fit compared with model M1 (based on visual inspection and the AKA criterion; see also Figures 3 and 4 for all choices of number of breakpoints  $>2$ ). The optimal number of breakpoints for  $A_d$  according to the AKA criterion was 3, indicating that for these data, the systematic deviation is not too complex.

The upper panel of Figures 3 and 4 show the data and the empirical Bayes (posthoc) predictions of models M1 (dotted line) and M2 (solid line) for *R*- and *S*-oxybutynin, respectively, for subjects

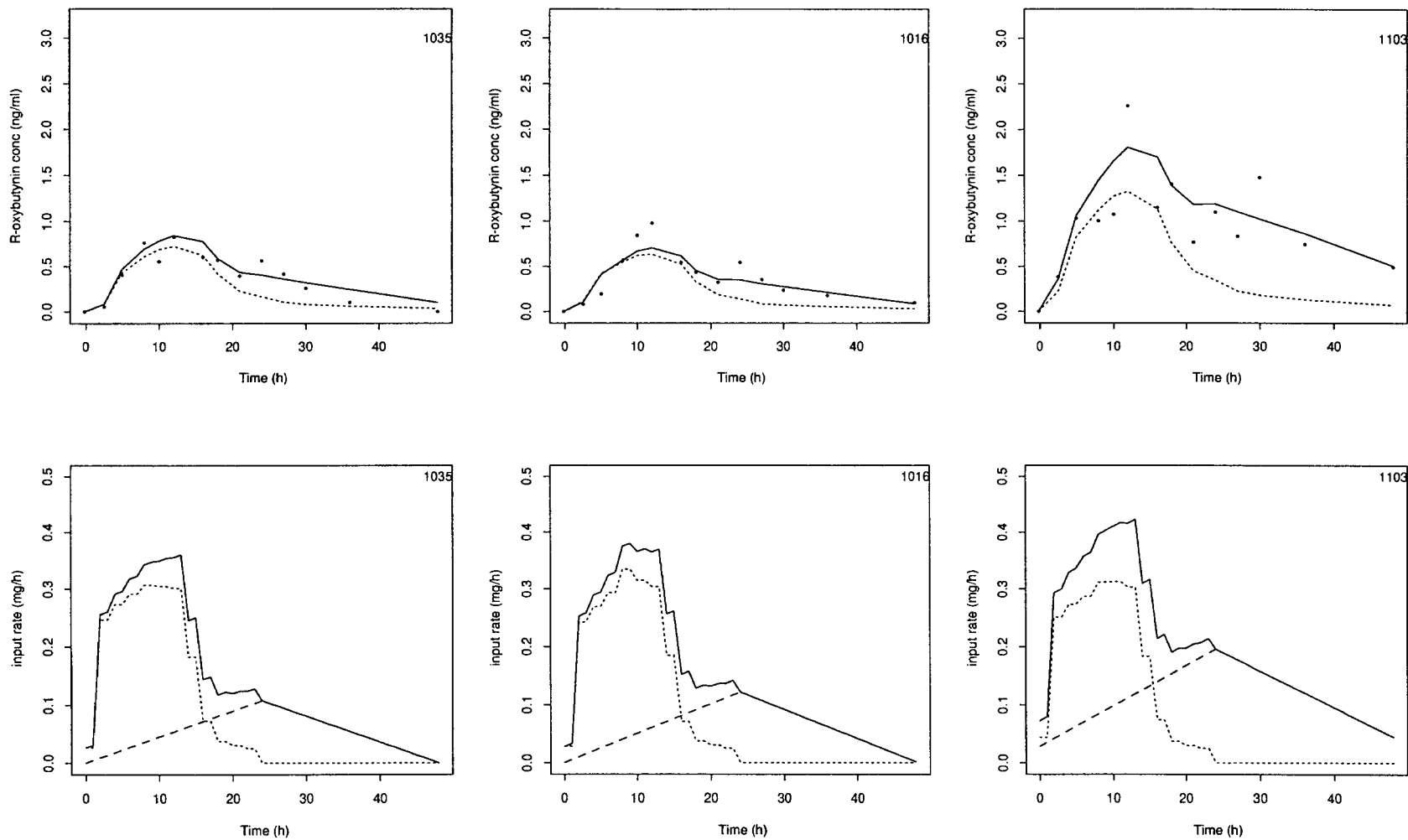


**Figure 3.** Selected individual subjects of models M1 and M2 to dataset *R-1\_A*, and input functions for model M2. Left, center, and right panels represent good, average, and poor fits (see text), respectively. Upper panels: (dots) observations; (dotted and solid lines) predictions of models M1 and M2, respectively. Lower panels are the estimated input function for model M2: (solid, dotted, and dashed lines correspond to  $A_{vivo} = A_{vitro} + A_d$ ,  $A_{vitro}$ , and  $A_d$ , respectively).

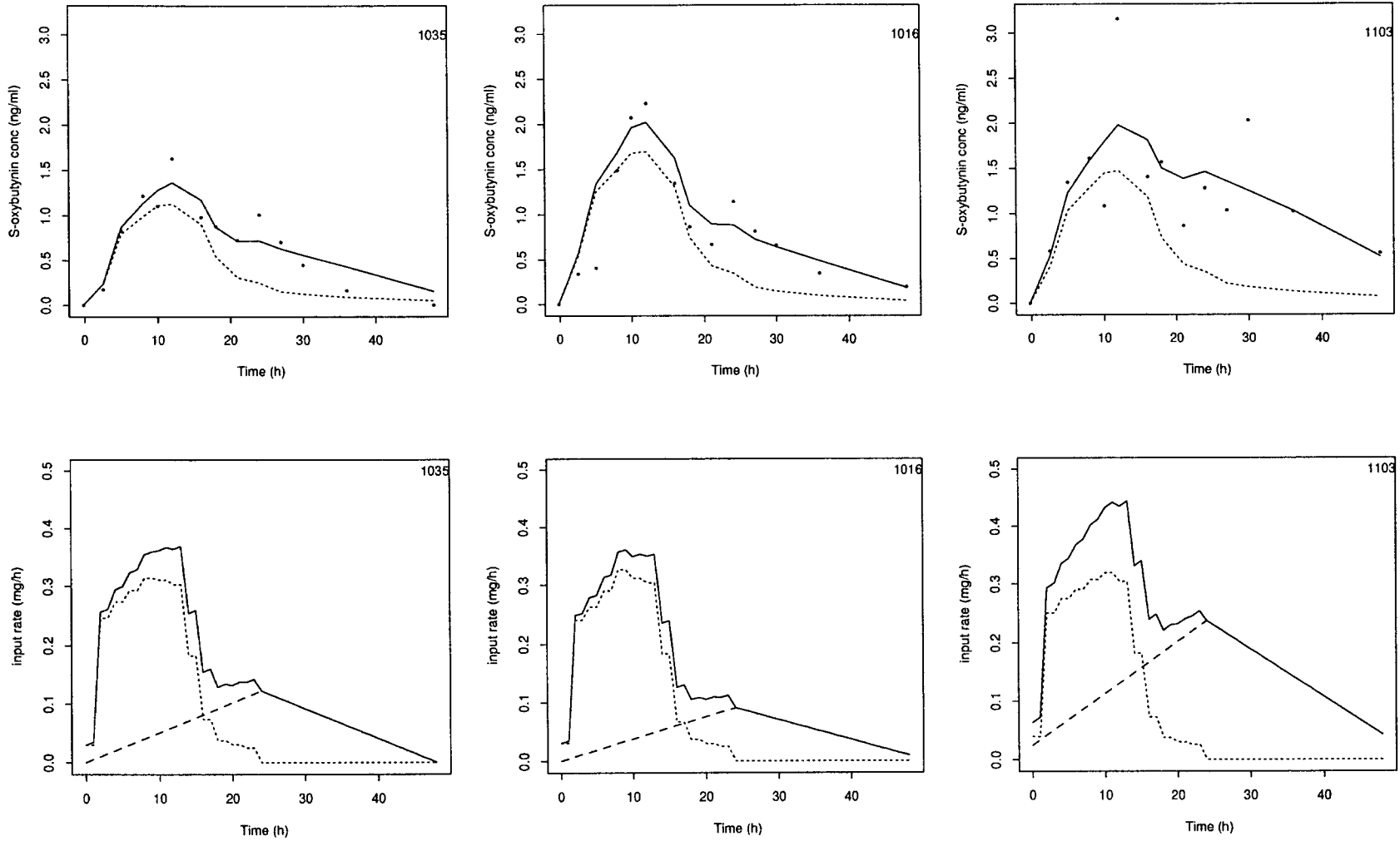


**Figure 4.** Selected individual subjects of models M1 and M2 to dataset S-1\_A and input functions for model M2. See legend to Figure 3 for key to symbols.

**Table 1.** Estimated Total Inputs and Bioavailability for Study A: *R*- and *S*-Oxybutynin<sup>a</sup>

Dataset	Model	$A_D$	$A_{VITRO}$	$A_{VIVO}$	BIO
<i>R</i> -1_A	M1	—	4.29	4.29	0.86
<i>R</i> -1_A	M2	3.79 (2.40)	4.21 (0.11)	8.00 (2.43)	1.60 (0.48)
<i>S</i> -1_A	M1	—	4.28	4.28	0.86
<i>S</i> -1_A	M2	4.76 (2.51)	4.20 (0.09)	8.96 (2.87)	1.79 (0.57)
<i>R</i> -2_A	M1	—	4.29	4.29	0.86
<i>R</i> -2_A	M2	3.32 (2.23)	4.12 (0.1)	7.45 (2.19)	1.49 (0.44)
<i>S</i> -2_A	M1	—	4.29	4.29	0.86
<i>S</i> -2_A	M2	4.01 (2.40)	4.22 (0.53)	8.23 (2.49)	1.65 (0.50)
<i>R</i> -3_A	M1	—	4.43	4.43	0.89
<i>R</i> -3_A	M2	4.29 (3.72)	4.30 (0.12)	8.59 (3.78)	1.72 (0.77)
<i>S</i> -3_A	M1	—	4.44	4.44	0.89
<i>S</i> -3_A	M2	5.45 (4.22)	4.34 (0.13)	9.78 (4.30)	1.96 (0.83)

<sup>a</sup>Standard deviations in parentheses.

with a good, average, and poor fit (selected using the 10, 50, and 90% quantiles, respectively, of the sum of weighted squared residuals corresponding to model M2). Note how model M1 systematically underestimates drug concentrations (in particular after 24 h where it can only predict zero input). The lower panels of the same figures present the corresponding input rates for model M2 (dotted line:  $A_{vitro}$ ; dashed line:  $A_d$ ; solid line:  $A_{vivo} = A_{vitro} + A_d$ ). Similar results are obtained for data sets *R*-2\_A, *R*-3\_A, *S*-3\_A. Model M2 significantly improves the fit for both the *R*- and *S*-enantiomers.

The estimated total inputs and relative bioavailability for all the data sets are reported in Table 1. The total *in vivo* input ( $A_{VIVO}$ ) estimated by model M2 for data sets *R*-1\_A, *R*-2\_A, and *R*-3\_A is 86, 72, and 92%, respectively, values that

higher than the actual *in vitro* released amount of each enantiomer. The contributions  $A_d$  to the total *R*-oxybutynin input are 48, 44, and 49% of the total. The estimates obtained by model M2 for the *R*-enantiomer are very similar for the three data sets. For *S*-oxybutynin,  $A_{VIVO}$  is estimated higher than that of the *R*-enantiomer; that is 110, 92, and 123% higher than the *in vitro* released amount for data sets *S*-1\_A, *S*-2\_A, and *S*-3\_A, respectively. The contribution to the total by  $A_D$  for *S*-oxybutynin is 53, 48 and 56%, respectively. The estimated total inputs and relative bioavailabilities for the *S*-enantiomer show more marked differences between the three data sets. However, the variability associated with these parameters seem to be greater for the *S*-enantiomer.

The estimated input rates for all the data sets are reported in Table 2. Model M2 predicts an *in*

**Table 2.** Estimated Input Rates for Study A: *R*- and *S*-Oxybutynin<sup>a</sup>

Dataset	Model	$A_{d,12}$	$A_{vitro,12}$	$A_{vivo,12}$	$A_{vivo,24}$
<i>R</i> -1_A	M1	—	0.31	0.31	—
<i>R</i> -1_A	M2	0.08 (0.08)	0.3 (0.00)	0.39 (0.09)	0.11 (0.05)
<i>S</i> -1_A	M1	—	0.31	0.31	—
<i>S</i> -1_A	M2	0.11 (0.11)	0.3 (0.00)	0.41 (0.11)	0.15 (0.05)
<i>R</i> -2_A	M1	—	0.31	0.31	—
<i>R</i> -2_A	M2	0.08 (0.07)	0.3 (0.00)	0.38 (0.07)	0.12 (0.06)
<i>S</i> -2_A	M1	—	0.31	0.31	—
<i>S</i> -2_A	M2	0.09 (0.07)	0.3 (0.00)	0.39 (0.08)	0.11 (0.08)
<i>R</i> -3_A	M1	—	0.28	0.28	—
<i>R</i> -3_A	M2	0.09 (0.1)	0.28 (0.01)	0.36 (0.1)	0.15 (0.10)
<i>S</i> -3_A	M1	—	0.28	0.28	—
<i>S</i> -3_A	M2	0.13 (0.12)	0.28 (0.01)	0.41 (0.12)	0.19 (0.13)

<sup>a</sup>Data are given in mg/h (standard deviations).

**Table 3.** Estimated Total Inputs and Bioavailability for Studies A, B, and C: *R*-Oxybutynin (Model M3)<sup>a</sup>

Dataset	$A_D$	$A_{VITRO}$	$A_{VIVO}$	BIO
<i>R</i> -1_A	4.10 (3.26)	4.23 (0.18)	8.33 (3.38)	1.67 (0.68)
<i>R</i> -2_A	3.60 (3.14)	4.17 (0.12)	7.77 (3.22)	1.55 (0.64)
<i>R</i> -3_A	4.23 (2.94)	4.39 (0.31)	8.62 (3.14)	1.72 (0.63)
<i>R</i> -1_B	2.65 (.39)	4.26 (0.41)	6.91 (1.72)	1.38 (0.34)
<i>R</i> -2_B	2.90 (2.07)	4.37 (0.2)	7.27 (2.19)	1.45 (0.44)
<i>R</i> -3_B	5.67 (3.3)	8.47 (0.59)	14.14 (3.82)	1.41 (0.38)
<i>R</i> -1_C	2.42 (1.35)	4.15 (0.15)	6.57 (1.46)	1.31 (0.29)
<i>R</i> -2_C	2.65 (1.4)	4.22 (0.22)	6.86 (1.55)	1.37 (0.31)

<sup>a</sup>Standard deviations in parenthesis.

*in vivo* input rate at 12 h ( $A_{vivo,12}$ ) that is 26, 23, and 32 % higher than the *in vitro* release rate for data sets *R*-1\_A, *R*-2\_A and *R*-3\_A, respectively, and 35, 26 and 46% higher than the *in vitro* for data sets *S*-1\_A, *S*-2\_A, and *S*-3\_A respectively. The *in vivo* input rates ( $A_{vivo,24}$ ) are always positive at 24 h, and the model predicts an *in vivo* delayed input that continues up to 48 h.

#### Further Validation (Test Data Set Cross Validation)

Although  $A_d$  is of low dimension (indicating no overparametrization of the model), to further validate the estimated  $A_d$  we used the data sets *R*-1\_A, *R*-2\_A, and *R*-3\_A as test data sets for each other. To do so, the results obtained in the *R*-1\_A study were used to predict *R*-2\_A and *R*-3\_A; similarly, *R*-2\_A was used to predict *R*-1\_A and *R*-3\_A was used to predict *R*-1\_A and *R*-2\_A. As measure of predictive performance, we computed the summary parameters for drug absorption (total input and input rates) and for drug concentrations (area under the curve and peak concentration) using  $A_d$  and  $\Omega_d$  (and  $A_{vitro}$  and  $\Omega_{vitro}$ ) estimated from one data set to predict the others. In all cases, we obtained similar results to the ones reported in Tables 1 and 2 (within few percent differences), indicating that estimated  $A_d$  are predictive of *in vivo* release. Accordingly, and not surprising, plasma oxybutynin concentrations are also well predicted, as measured by the AUC and peak concentration statistics. These results further indicate that (for oxybutynin) the function  $A_d$  can be used, combined with the *in vitro* release function, to provide consistent IVIVC-type predictions within the study used to estimate it, and, importantly, across studies. The test data cross validation further indicates that in this context,

the AKA selected a satisfactory dimension (number of parameters) for  $A_d$ .

#### In Vivo Input Function (OROS Data, Studies B and C)

In Studies B and C, the IR disposition function is only available as a population mean (obtained from Study A). To deal with this situation we used model M3, which (as detailed in the Method Section, subsection estimation) estimates  $A_d$  conditional on the mean IR disposition function (and  $A_{vitro}$ ,  $\Omega_{vitro}$ ). To validate this approach we also fit model M3 to the data from Study A.

Model M3 described most subjects adequately (not shown) and confirmed the existence of an apparent “delayed” input resulting in the otherwise unexplainable sustained concentrations after 20 h from the OROS dose. The total input and relative bioavailabilities obtained for the *R*-enantiomer in Studies A, B, and C are shown in Table 3. The total input values obtained for Study A can be compared with the values reported in Table 1 (where individual estimates of the IR disposition function were used). The values are very similar, yet, as expected, the standard deviations of the estimates increase. This increase gives an indication that estimates of  $A_d$  are predictive of *in vivo* input when individual IR disposition functions are not available. The values obtained for Studies B and C are also reasonable and close to the values obtained by Study A.

## DISCUSSION

In this paper we present a further elaboration and application of a general model describing IVIVC presented by Verotta<sup>3</sup> (where the method is tested

using simulations). The model allows the *in vivo* input to differ in a systematic way from the *in vitro* to account for change in the *in vivo* release. Limited assumptions on the departure from the *in vitro* release are made, allowing a wide range of possible situations to be taken into account. The extent of departure from the *in vitro* release pattern is established using a statistical model selection criterion. The model incorporates random effects describing both the *in vitro* release rates variability and interindividual variability in the systematic deviation from *in vitro* release, thus providing a general semiparametric population model for IVIVC. The model is useful because it can overcome and quantify the lack of IVIVC using a relatively simple descriptive methodology, which, as we have shown, allows for reliable predictions across studies. This predictive performance might be apparently surprising, but it is consistent with the predictive performance of other semiparametric or nonparametric methods: If the assumptions of our model (pharmacokinetics, linearity, and time invariance) are not violated, the method is expected to perform well. The method we propose takes great care in determining the flexibility of the  $A_d$ ; that is, its number of parameters. When  $A_d$  is too flexible (high number of parameters), one should expect a really good fit of the data but unreliable predictions of validation data sets (one can always obtain a perfect, interpolating fit when using empirical functions, but then prediction of validation data suffers). When  $A_d$  is "just right," the fit is (compared with an interpolation) less good, but reliable predictions of validation data sets are expected. This situation is the same, in the much more complicated IVIVC setting, as the classic bias/variance tradeoff one finds in nonparametric regression; for example, using a smoothing function.<sup>15</sup>

The data considered in this paper showed a peculiar form of lack of IVIVC. High concentrations of *R*- and *S*-oxybutynin were observed between 20 and 48 h after OROS administration, whereas according to the *in vitro* release data, most of the drug should be released after 16 h from administration. A severe misfit of the observed concentrations resulted when the  $A_{\text{vitro}}$  was used as input. This pattern is consistent in all cases of OROS administration (fasted or fed, therefore, it seems not to be affected by gastric emptying; total dose, 10 versus 20 mg; and different formulations, 10 versus 5 mg), and resulted in an apparently higher relative bioavailability

of the OROS oxybutynin formulation relative to the IR.

We are able to address this apparent lack of IVIVC (and therefore predict *in vivo* concentration based on *in vitro* release rate) using a relatively simple form of systematic deviation from the *in vitro* release (see lower panels of Figures 3 and 4). The profile of  $A_d$  is consistent in all cases of OROS administration: (i) fasted or fed (suggesting  $A_d$  is not affected by gastric emptying), (ii) total dose of 10 or 20 mg, and (iii) different formulations (10 versus 5 mg).

The modeling of Studies B and C shows a possible way to obtain IVIVC for cases where individual estimates of disposition are not available. The proposed model (M3) obtains IVIVC conditional on the population mean IR disposition. This method is validated using Study A (where IR disposition is measured) and appears to obtain satisfactory results. We will, however, investigate further model M3 to take into account intersubject variability in the disposition function. As a word of caution, we note that in different situations<sup>16</sup> it was noticed that multiple fonts of variability could induce a non-unique solution to a population estimation problem, and partly invalidate its results.

Although the modeling of the data is successful, from a physiological point of view the observed OROS data are difficult to explain. The absolute bioavailability of oxybutynin when administered orally as an IR form or a solution is stated to be quite low, ~6%.<sup>8</sup> Therefore, even a small increase in the amount absorbed can easily result in almost doubling the bioavailability of a formulation relative to the IR form. The reason for this low bioavailability is postulated to be extensive first-pass metabolism in the gut wall. Following OROS, the drug is mainly released in the colon. Because the concentration of the metabolizing enzymes is smaller in the colon, it is possible that oxybutynin released from the OROS form in that location undergoes a less extensive biotransformation. However, although this hypothesis may provide an explanation for the additional apparent input estimated in this analysis, it cannot predict the late profile after 20–24 h.

In conclusion, the model we proposed represents a general strategy for establishing IVIVC or predicting future studies once IVIVC is established. The approach is an empirical one based on linear system theory and deconvolution: it introduces a function to take into account systematic temporal variation between *in vitro* and *in vivo*

release, and couples the representation with a sophisticated estimation strategy.

## SOFTWARE AVAILABILITY

The computer code used to implement the approach is available from one of the authors (Verotta) upon request.

## ACKNOWLEDGMENTS

This work was supported by NIH Grant GM 51197 and by Alza Corporation.

## REFERENCES

1. Young D, Devane J, Butler J, editors. 1997. *In vivo-in vitro* relationships. New York: Plenum Press.
2. Langenbucher F. 1982. Numerical convolution/deconvolution as a tool for correlating *in vitro* with *in vivo* drug availability. *Pharm Ind* 44:1166–1172.
3. Verotta D. 1997. A general framework for non-parametric subject-specific and population deconvolution methods for *in vivo-in vitro* correlation. In: Young D, Devane J, Butler J, editors. *In vivo-in vitro* relationships. New York: Plenum Press.
4. Gupta SK, Shah J, Sathyan G. 1997. Evidence for site specific presystemic metabolism of oxybutynin following oral administration. *Clin Pharm Ther* 61:227.
5. Sathyan G, Ho P, Gupta SK. 1998. Stereospecific pharmacokinetics of once-daily controlled release oxybutynin: Dose proportionality. *Pharm Res S-484*.
6. Sathyan G, Natarajan S, Gupta SK. 1998. Stereospecific pharmacokinetics of once-daily controlled release oxybutynin: Comparison with immediate release formulation and effect of food. *Pharm Res S-481*.
7. Verotta D. 1996. Concepts, properties, and applications of linear systems to describe the distribution, identify input, and control endogenous substances and drugs in biological systems. *Crit Rev Bioeng* 24:73–139.
8. Douchamps J, Derenne F, Stockis A, Gangji D, Juvent M, Herchuelz A. 1988. The pharmacokinetics of oxybutynin in man. *Eur J Clin Pharmacol* 35:515–520.
9. Verotta D. 1995. New approaches to self-modeling non-linear regression. In: D'Argenio DZ, editor. *Advanced methods of pharmacokinetic and pharmacodynamic system analysis II*. New York: Plenum.
10. DeBoor C. 1978. *A practical guide to splines*. New York: Springer-Verlag.
11. Beal SL, Sheiner LB. 1992. *NONMEM users guide, part VII; Conditional estimation methods*. Division of Clinical Pharmacology, University of California at San Francisco.
12. Akaike H. 1974. A new look at the statistical model identification problem. *IEEE Trans Automat Contr* 19:716–723.
13. Schwarz G. 1978. Estimating the dimension of a model. *Ann Statist* 6:461–464.
14. Hannan EJ. 1987. Rational transfer function approximation. *Statist Sci* 2:1029–1054.
15. Craven P, Wahba G. 1979. Smoothing noisy data with spline functions. *Numer Math* 31:377–403.
16. Fattinger KE, Verotta D. 1995. Estimating bioavailability when clearance varies with time: The effect of model misspecification. *Clin Pharm Ther* 58:595–600.